Cell Transplantation
2018, Vol. 27(2) 285-298

DOI: 10.1177/0963689717721514
journals.sagepub.com/home/cll
SAGE

Cardiotrophic Growth Factor–Driven Induction of Human Muse Cells Into Cardiomyocyte-Like Phenotype

Mohamed Amin[1,2], Yoshihiro Kushida[1], Shohei Wakao[1], Masaaki Kitada[1], Kazuki Tatsumi[1,3], and Mari Dezawa[1]

Abstract

Multilineage-differentiating stress-enduring (Muse) cells are endogenous nontumorigenic stem cells collectable as stage-specific embryonic antigen 3 (SSEA-3) + from various organs including the bone marrow and are pluripotent-like. The potential of human bone marrow-derived Muse cells to commit to cardiac lineage cells was evaluated. We found that (1) initial treatment of Muse cells with 5′-azacytidine in suspension culture successfully accelerated demethylation of cardiac marker Nkx2.5 promoter; (2) then transferring the cells onto adherent culture and treatment with early cardiac differentiation factors including wingless-int (Wnt)-3a, bone morphogenetic proteins (BMP)-2/4, and transforming growth factor (TGF) β1; and (3) further treatment with late cardiac differentiation cytokines including cardiotrophin-1 converted Muse cells into cardiomyocyte-like cells that expressed α-actinin and troponin-I with a striation-like pattern. MLC2a expression in the final step suggested differentiation of the cells into an atrial subtype. MLC2v, a marker for a mature ventricular subtype, was expressed when cells were treated with Dickkopf-related protein 1 (DKK-1) and Noggin, inhibitors of Wnt3a and BMP-4, respectively, between steps (2) and (3). None of the steps included exogenous gene transfection, making induced cells feasible for future clinical application.

Keywords

cardiomyocyte, cardiotrophin-1, suspension culture, nontumorigenic cells, pluripotency

Introduction

Cardiovascular disorders are the leading cause of death of noncommunicable diseases, and cell therapy is becoming one of the trends for treatment in this field[1]. The most general stem cells for clinical use might be mesenchymal stem cells (MSCs) because of their easy accessibility and safety. They show a broad spectrum of differentiation potentials across oligolineage boundaries between mesodermal and endodermal, as well as ectodermal lineages whereas the differentiation rate is usually not high, suggesting that a small subpopulation of MSCs are playing a role in this transdifferentiation[2]. MSCs are a heterogenous population because they are usually collected simply as adherent cells, and a universal surface antigen for their isolation has not been identified[3].

Within the MSC population, we previously identified multilineage-differentiating stress-enduring (Muse) cells as considerable percentage of total MSCs, which can be isolated as cells positive for a pluripotent stem cell surface marker: stage-specific embryonic antigen (SSEA)-3[2]. They can generate cells representative of all 3 major lineages from a single cell, self-renew, express pluripotency genes, and show triploblastic differentiation, suggesting their pluripotency[4]. Various reports have shown that Muse cells can differentiate into ectodermal cells such as melanocytes[5], epidermal cells[6], and neuronal cells[7,8]; endodermal cells represented by hepatocytes and cholangiocytes[9,10]; and into mesodermal cells such as osteocytes, adipocytes[11], and skeletal muscle cells[4]. Adipose-derived Muse cells have also shown spontaneous triploblastic differentiation ability[12].

[1] Department of Stem Cell Biology and Histology, Tohoku University Graduate School of Medicine, Sendai, Japan
[2] Department of Biochemistry, Faculty of Pharmacy, Mansoura University, Mansoura, Dakahlia, Egypt
[3] Life Science Institute Inc., Regenerative Medicine Division, Nagoya, Japan

Submitted: March 20, 2017. Revised: May 12, 2017.
Accepted: May 18, 2017.

Corresponding Author:
Mohamed Amin and Mari Dezawa, Department of Stem Cell Biology and Histology, Tohoku University Graduate School of Medicine, 2-1 Seiryo-machi, Aoba-Ku, Sendai, Miyagi 980-8575, Japan.
Emails: amin@med.tohoku.ac.jp; mdezawa@med.tohoku.ac.jp

Notably, cells negative for SSEA-3 among MSCs, namely, non-Muse cells that correspond to the vast majority of MSCs, do not show such a broad spectrum of differentiation[4]. Promoter regions of octamer-binding transcription factor 3/4 (Oct3/4) and Nanog are highly methylated in non-Muse cells as compared to those of Muse cells, and accordingly, gene expression levels relevant to pluripotency are substantially lower than those in Muse cells. Furthermore, non-Muse cells are not capable of self-renewal, nor do they show differentiation into ectodermal or endodermal lineages even in the presence of appropriate induction cytokines; these are stark differences between Muse and non-Muse cells[11,13]. Moreover, Muse cells have shown an anti-inflammatory effect by down-regulating tumor necrosis factor-α (TNF) and immune-modulatory effects via spontaneously expressing transforming growth factor β (TGF-β1)[14]. For these reasons, Muse cells are suggested to be a better material for generation of cells for transplantation therapy than a crude MSC population.

Cardiomyocytes are terminally differentiated cells that lack the ability to proliferate[15]. They have a unique cytoskeleton containing several contractile proteins represented by actin, myosin, titin, troponin, and α-actinin that are arranged into sarcomeres[16]. In addition, intercellular connections through gap junction channels, mainly composed of connexin 43, allow cardiomyocytes to couple electrochemically and to contract synchronously[17].

Various kinds of factors and signaling pathways are known to regulate cardiac differentiation during normal development. Bone morphogenetic proteins (BMPs), wingless-int (Wnt)[18], and TGF-β families are key factors that regulate cardiogenesis in a context-dependent manner[19]. In addition, basic fibroblast growth factor (bFGF) participates in the orchestration of cardiac differentiation[20]. Cardiotrophin-1—member of the interleukin (IL)-6 family—was originally identified as a marker of cardiac hypertrophy[21], but later it was found to be cardioprotective[22] and is even known to induce differentiation toward the cardiac lineage in MSCs[23] and embryonic stem cells (ESCs)[24].

MSCs have been studied for possible regeneration of damaged areas in acute heart conditions via a transplant or intravenous injection. In chronic conditions, however, there may be less chance for stem cells to differentiate into target cells due to a severely hostile microenvironment and damage to the built-in regenerative system. In such a case, injection or transplant of already differentiated stem cell–derived cardiomyocytes may be beneficial. In the present article, we explored the potential of Muse cells to differentiate in vitro into cells with cardiomyocyte characteristics by means of a combination of suspension culture and multistep cytokine induction.

Materials and Methods

Fluorescence-Activated Cell Sorting (FACS) Isolation of SSEA-3+ Muse Cells

Human bone marrow-derived MSCs (BM-MSCs) were purchased from Lonza . The cells were cultured in Dulbecco's modified Eagle's medium (DMEM) low glucose (10567-014; Gibco, Grand Island, NY, USA) containing 10% of fetal bovine serum (FBS) and 2 ng/μL bFGF (Wako, Saitama, Japan). We stained MSCs (from passage 1 to passage 4) with acidic β-galactosidase using a senescent cell histochemical staining kit (Sigma-Aldrich, St. Louis, MO, USA) to determine the passage number to be adopted in the article. For collection of Muse cells, MSCs were incubated with a rat anti-SSEA-3 IgM antibody (1:100 dilution; Millipore, Billerica, MA, USA) and stained with a secondary antibody: a fluorescein isothiocyanate-conjugated antirat IgM antibody (1:100; Jackson ImmunoResearch Laboratories, Inc., West Grove, PA, USA) as described previously[4]. The SSEA-3+ fraction was sorted by means of a BD FACS Aria™ II cell sorter (Becton Dickinson, San Jose, CA, USA). The sorted fraction was cultured overnight with DMEM low glucose containing 10% of FBS and 2 ng/μL bFGF and then was used for cardiomyocyte induction.

Cell Culture and Cytokine Cocktails for Induction

Muse cells were divided into 3 groups and were subjected to each induction scheme as described in Fig. 1.

Adherent group. Muse cells were plated at $1.55 \times 10^4/cm^2$ and cultured in the adherent state for the entire period of induction on a laminin-coated surface. The cells were first incubated with DMEM low glucose containing 2% of FBS plus TGF-β1 (2.5 ng/mL, Wako), BMP-4 (5 ng/mL, Wako), BMP-2 (5 ng/mL, Sigma-Aldrich), activin A (10 ng/mL, Wako), Wnt-3a (50 ng/mL, R&D Systems, Minneapolis, MN, USA), and bFGF (10 ng/mL, Wako) for 7 d and then for 2 wk with DMEM low glucose containing 2% of FBS plus TGF-β1, insulin-like growth factor-1 (IGF-1, 5 ng/mL, Sigma-Aldrich), hepatocyte growth factor (HGF; 20 ng/mL, Wako), and cardiotrophin-1 (CT-1; 200 ng/mL, Sigma-Aldrich).

Sus+Ad group. Muse cells were first cultured in suspension in DMEM low glucose, 10% of FBS, 2 ng/μL bFGF, and 10 μM 5′-azacytidine (5′-AZA; Sigma-Aldrich) in a poly(2-hydroxyethyl methacrylate) (P3932; Sigma-Aldrich)-coated 24-well plate prepared as described previously[2] at 3×10^4/well in order to form Muse cell aggregates. After 3 d, the aggregates were transferred to adherent culture, kept overnight to allow the aggregates to attach to the culture dish, and then were treated as described for the adherent group.

Sus+Ad+DN group. The protocol is the same as that of the Sus+Ad group except that incubation with Noggin (100 ng/mL, R&D Systems) and Dickkopf-related protein 1 (DKK-1; 50 ng/mL, R&D Systems) in DMEM low glucose plus 2% of FBS for 2 d was inserted between the 2 incubation steps (Fig. 1).

During the induction, the medium was changed every 2 d. The cells were properly trypsinized and subcultured

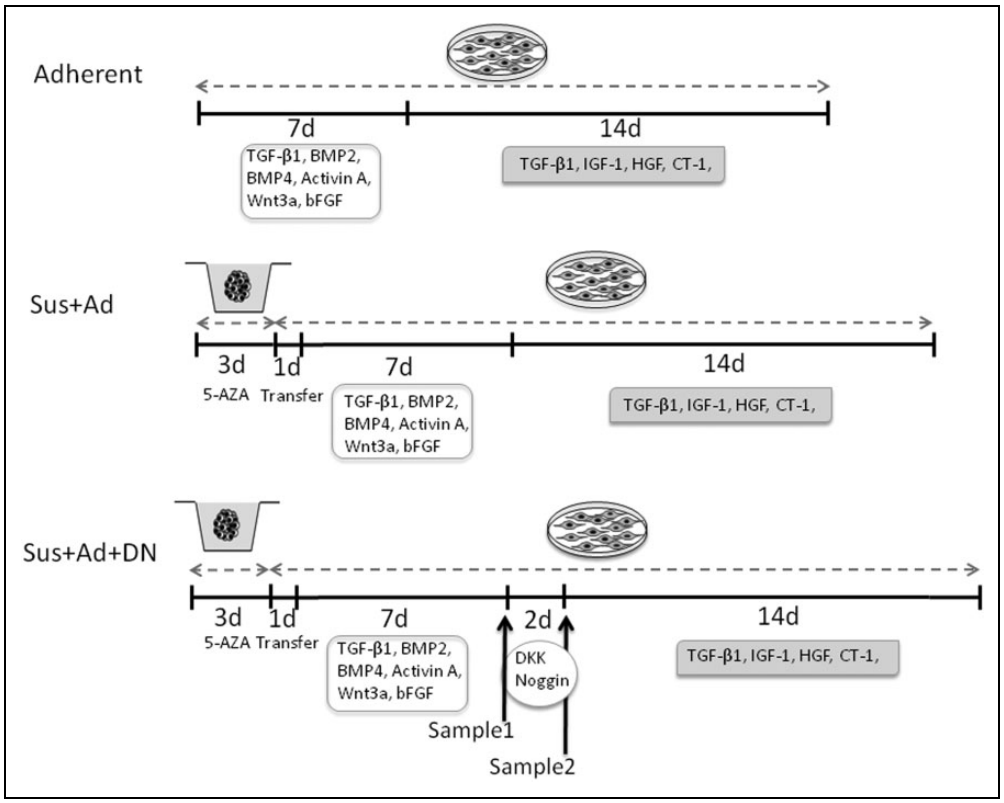

Fig. 1. Induction time line of the adherent, Sus+Ad, and Sus+Ad+DN groups, sample 1, and sample 2; TGF-β1 (transforming growth factor-1), BMP2/4 (bone morphogenetic protein 2/4), bFGF (basic fibroblast growth factor), IGF-1 (insulin-like growth factor-1), HGF (hepatocyte growth factor), CT-1 (cardiotrophin-1), 5′-azacytidine (5′-AZA).

whenever they reached nearly 100% confluence except for the last 2 wk of induction.

Reverse Transcription–Polymerase Chain Reaction (RT-PCR)

Total RNA was extracted from the induced cells on the last day of induction by means of the NucleoSpin RNA XS kit (Macherey-Nagel, Düren, Germany). Then, 400 ng of RNA was used for cDNA synthesis using SuperScript VILO (Invitrogen, Waltham, MA, USA). cDNA was used for Taq polymerase PCR using the primers (Table 1) for GATA-4, Tbx20, atrial natriuretic peptide (ANP), Nkx2.5, MLC1v[25], MLC1a[26], HCN-4[27], Myo-D[28], and β-actin. Human fetal heart RNA (Clontech Laboratories, Inc., Mountain View, CA, USA) served as positive control for GATA-4, Tbx20, ANP, HCN-4, and Nkx2.5. Human adult heart RNA (Clontech Laboratories, Inc.) was used as positive control for MLC1v and MLC1a. Human adult skeletal muscle RNA (Clontech Laboratories, Inc.) served as positive control for Myo-D. Human adult liver RNA (Clontech Laboratories, Inc.) was used as a negative control for all markers except Tbx20, ANP, and GATA-4. Human dermal fibroblast RNA (Clontech Laboratories, Inc.) served as negative a control for Tbx20 and ANP, and human adult brain RNA (Clontech Laboratories, Inc.) for GATA-4. The amplification program included the initial denaturation step at 94°C for 5 min followed by 40 cycles of denaturation at 94°C for 30 s, annealing at T_m for 30 s, and extension at 72°C for 30 s; then the final extension step at 72°C for 10 min. For GATA-4, Tbx20, and Myo-D, the denaturation, annealing, and extension intervals were 1 min instead of 30 s, and the final extension step lasted at 7 min instead of 10 min.

Quantitative PCR (Q-PCR)

Total RNA was extracted from the induced cells on the final day of induction by means of the NucleoSpin RNA XS Kit (Macherey-Nagel). In addition, total RNA from "sample 1" and "sample 2" of the Sus+Ad+DN group was also collected (Fig. 1). Then, 100 ng of total RNA was used for cDNA synthesis using the SuperScript VILO kit (Invitrogen). GATA-4 (Hs00171403_m1), α-actinin (Hs00153809_m1), MLC2a (Hs00221909_m1), MLC2v (Hs00166405_m1), and HCN4 (Hs00975492_m1) expression levels were analyzed by the ΔΔCT method with the AB systems 7500 Fast real-time PCR (Applied Biosystems, Foster City, CA, USA) according to the manufacturer's instructions. β-Actin (Hs99999903_m1) served as an endogenous control. For MLC2a and MLC2v analyses, 2 additional groups for the Sus+Ad+DN group in which either CT-1 or HGF was removed from the induction, named, as

Table 1. Primers Used for Reverse Transcription–Polymerase Chain Reaction Experiments.

Marker		Sequence	T_m (°C)	Product Size (bp)
GATA-4	F (5′→3′)	CCAATCTCGATATGTTTGACGACT	63.6	316
	R (5′→3′)	TTTGGATCCCCTCTTTCCGC		
Tbx20	F (5′→3′)	CCAAATCGAGGGTCAGCCTT	69	294
	R (5′→3′)	GGGCCCCTGCTGAAAATAGT		
Atrial natriuretic peptide	F (5′→3′)	GAACCAGAGGGGAGAGACAGAG	66	406
	R (5′→3′)	CCCTCAGCTTGCTTTTTAGGAG		
NKx2.5	F (5′→3′)	GGGACTTGAATGCGGTTCAG	54	289
	R (5′→3′)	CTCATTGCACGCTGCATAATC		
MLC1v	F (5′→3′)	GAGGTCGAGTTTGATGCTTCC	56.4	300
	R (5′→3′)	CGAAGTCCTCATAGGTGCCTG		
MLC1a	F (5′→3′)	GGAGAGATGAAGATCACCTACGG	58.8	189
	R (5′→3′)	GGTGCCCTGCTCCTTGTTGC		
Myo-D	F (5′→3′)	AGCACTACAGCGGCGACT	60	266
	R (5′→3′)	GCGACTCAGAAGGCACGTC		
β-actin	F (5′→3′)	AGGCGGACTATGACTTAGTTGCGTTACACC	58.8	219
	R (5′→3′)	AAGTCCTCGGCCACATTGTGAACTTTG		

the Sus+Ad+DN(-CT) and Sus+Ad+DN(-HGF) groups, respectively.

For experiments on expression of pluripotency genes, we prepared 3 subsets: the naive adherent Muse, naive suspension Muse, and naive suspension Muse + 5-AZA. Naive adherent Muse cells were prepared directly from adherent culture. Naive suspension Muse + 5-AZA and naive suspension Muse were cultivated for 3 d in suspension culture as described earlier with or without 5′-AZA, respectively. Total RNA was extracted from the 3 subsets. Next, Pou5f1 (Hs04260367_gH), Sox-2(Hs01053049_s1), and Nanog (Hs042 60366_g1) expression levels were analyzed by the ΔΔCT method with β-actin as an endogenous control.

Naive adherent Muse were induced for 10 d under 4 different conditions in order to determine the main signaling pathway(s) involved in CT-1 cardiac induction effect. The 4 induction conditions were either; CT-1 only, CT-1 in presence of phosphatidyl inositol-3 kinase (PI3K) inhibitor (Ly294002, 10 μM, Calbiochem, La Jolla, CA, USA) (CT-1/PI3Ki), CT-1 in presence of mitogen activated protein kinase 1,2 (MEK1,2) inhibitor (U0126, 10 μM, Calbiochem) (CT-1/MEKi), or glycogen synthetase kinase 3 (GSK3) inhibitor only (CHIR99021, 10 μM, Wako) (GSK3i). After 10 d, α-actinin expression level was determined using the same conditions described above.

Global DNA Methylation

DNA was extracted from naive adherent Muse, naive suspension Muse, naive suspension Muse+5-AZA, and suspension Muse+5-AZA/adherent Muse (naive suspension Muse+5-AZA group transferred onto adherent culture overnight) by means of the QIAamp® DNA Mini Kit (Qiagen, Düsseldorf, Germany). The relative percentage of DNA methylation was determined using the Methylated DNA Quantification Kit (cat. #ab117128; Abcam, Cambridge, UK).

DNA Bisulfite Sequencing

DNA was extracted from naive adherent Muse, naive suspension Muse + 5-AZA, and sample 1 (Fig. 1) using QIAamp® DNA Mini kit. One microgram of DNA was treated with bisulfite using a MethylEasy™ Xceed Kit (cat. # ME002; Human Genetic Signatures, Sydney, Australia) according to the manufacturer's instructions. Primers were designed for a CpG island with 30 CpGs at Nkx2.5 proximal promoter[29]. Primers used were forward (5′-TGAGGGATAGGAAAAGTTTTAATATTAG-3′) and reverse (5′-ACAAATCTACCAAAATTTCAAAAAC-3′). Finally, ligation with pGEM-T Easy Vector System (Promega, Madison, WI, USA), bacterial transformation with *Escherichia coli* DH5α1, and sequencing with ABI 3500xL Genetic Analyzer (Life Technologies, Camarillo, CA, USA) was done.

Western Blot

Induced Muse cells were collected at the end point of induction in the adherent, Sus+Ad, and Sus+Ad+DN groups. Cell lysis was done by incubation for 15 min on ice with buffer containing 20 mM Tris–HCL, 1% Triton, 150 mM NaCL, and 1× protease inhibitor cocktail (Roche, Mannheim, Germany). Protein separation was done by 10% polyacrylamide gel (Supersep™ Ace, Wako), then transferred to a polyvinylidene difluoride (PVDF) membrane (0.45 μm Immobilon-P, Millipore). Blocking was done by incubation with 5% skim milk in TBST for 1 h with shaking at 4°C. The membrane was incubated with the primary antibody diluted in 1% skim milk overnight with shaking at 4°C, then washed with TBST 3 times each for 5 min at room temperature (RT). Then, the membrane was incubated with the secondary antibody diluted in 1% skim milk for 1 h with shaking at RT, followed by same washing step done after primary antibody incubation. Visualization of the membrane was done by chemiluminescence (Pierce ECL Plus, Thermo Fisher,

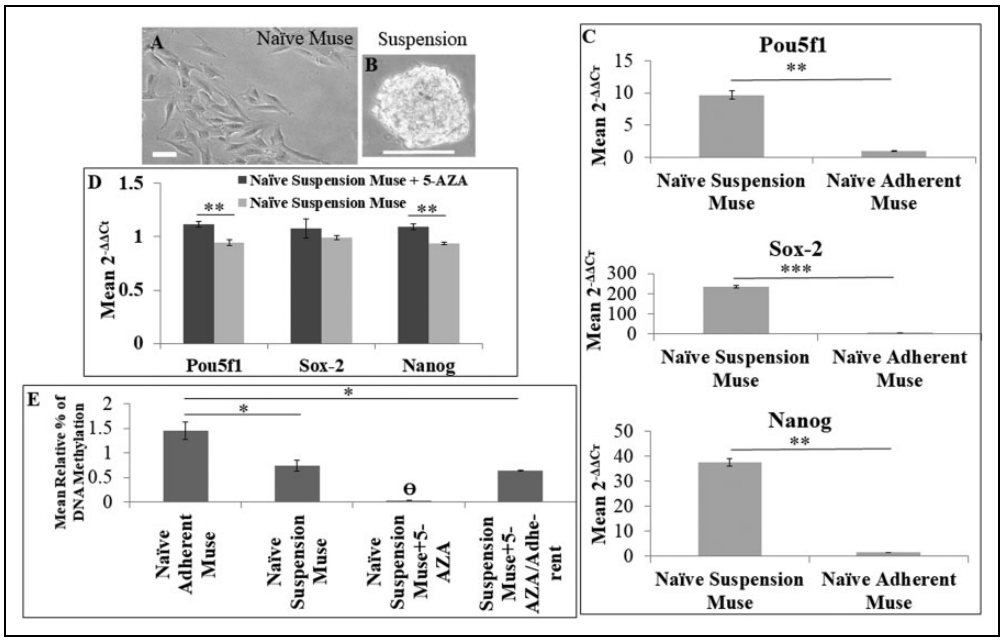

Fig. 2. Suspension culture and 5′-AZA increase Muse pluripotency. (A) Naive adherent Muse; (B) naive suspension Muse; (C) Q-PCR analysis of expression levels of pluripotency markers (Pou5f1, Sox-2, and Nanog) in naive suspension Muse versus naive adherent Muse; (D) Q-PCR analysis of expression levels of pluripotency markers (Pou5f1, Sox-2, and Nanog) in naive suspension Muse versus naive suspension Muse + 5-AZA; (E) relative percentage of DNA methylation in naive adherent Muse, naive suspension Muse, naive suspension Muse + 5-AZA, and suspension Muse + 5-AZA/adherent. *$P < 0.05$, **$P < 0.01$, ***$P < 0.001$. θ, under the detection level; 5′-AZA, 5′-azacytidine; Q-PCR, quantitative PCR; Muse, multilineage-differentiating stress-enduring. Scale bar: 100 μm. Pou5f1, POU class 5 homeobox 1; sex determining region Y-box 2, Sox-2; Nanog Homeobox, Nanog; Muse cells cultured in adherent, Naive Adherent Muse; Muse cells cultured in suspension, Naive Suspension Muse; Muse cells cultured in suspension in presence of 5′-azacytidine, Naive Suspension Muse + 5-AZA; Muse cells cultured in suspension in presence of 5′-azacytidine then moved to adherent culture overnight, Suspension Muse+5-AZA/Adherent.

Rockford, IL, USA), and the signals were quantified by ImageQuant LAS 4000 mini (GE Healthcare). Primary antibodies used were mouse anti α-actinin (Sigma-Aldrich; 1:700), mouse anti desmin (1:2,000; BD Pharmingen, San Diego, CA, USA), rabbit anti HCN4 (Abcam; 1:1,400), and mouse anti β-actin (Abcam; 1:7,000). Secondary antibodies were horseradish peroxidase (HRP)-conjugated goat anti-mouse IgG and HRP-conjugated goat anti-rabbit IgG (1:5,000; Jackson ImmunoResearch Laboratories, Inc.). Adult cardiomyocytes isolated from male, 9–wk-old Wistar rats as previously described were used as positive controls[30].

Immunocytochemistry

Muse cells from the adherent, Sus+Ad, and Sus+Ad+DN groups were fixed on the last day of induction by means of 4% paraformaldehyde (PFA) at 4°C for 2 h. Then, the cell samples were washed twice with phosphate-buffered saline (PBS). The cells were incubated with a block solution, which consisted of 20% Block Ace (DS Pharma Biomedical, Taito, Tokyo, Japan), 5% bovine serum albumin (BSA; Nacalai Tesque, Kyoto, Japan), and 0.3% Triton X-100 (Wako) in PBS for 2 h at 4°C. After the blocking, the samples were incubated with primary antibodies at 4°C overnight. Primary antibodies were the following: a mouse anti-troponin-I antibody (1:200 dilution; Chemicon), mouse anti α-actinin antibody (1:150 dilution; Sigma-Aldrich), and a rabbit anti-connexin 43 antibody (1:250 dilution; Abcam). The antibody diluent was the same as the block solution but with 5% Block Ace and 1% BSA. Then, the samples were washed 3 times for 5 min each at RT with PBS/Tween 20 (0.05%). Secondary antibodies were diluted with PBS/Triton X-100, and the cells were incubated for 1.5 h at RT. Secondary antibodies were the following: an Alexa 488-conjugated donkey antimouse antibody (Invitrogen) and an Alexa 568-conjugated donkey antirabbit antibody (Invitrogen) both at 1:1,000 dilution. After the secondary antibody incubation, 3 washes for 5 min each at RT were done. The cells were then counterstained with a 1:500 dilution of 4′,6-diamidino-2-phenylindole (DAPI) in PBS/Triton X-100 for 3 min followed by 3 washes for 5 min each at RT. Finally, the samples were mounted using the slowFade® Gold Antifade Mountant (Invitrogen) and were examined under a Nikon C2 Eclipse laser confocal microscope (Nikon, Tokyo, Japan). The percentage of troponin-I+ cells was calculated at the end point of the 3 induction groups using ∼2,000 cells for each group.

Statistical Analysis

Analysis of variance (ANOVA) followed by Tukey's post hoc test, and paired *t* test were employed for group

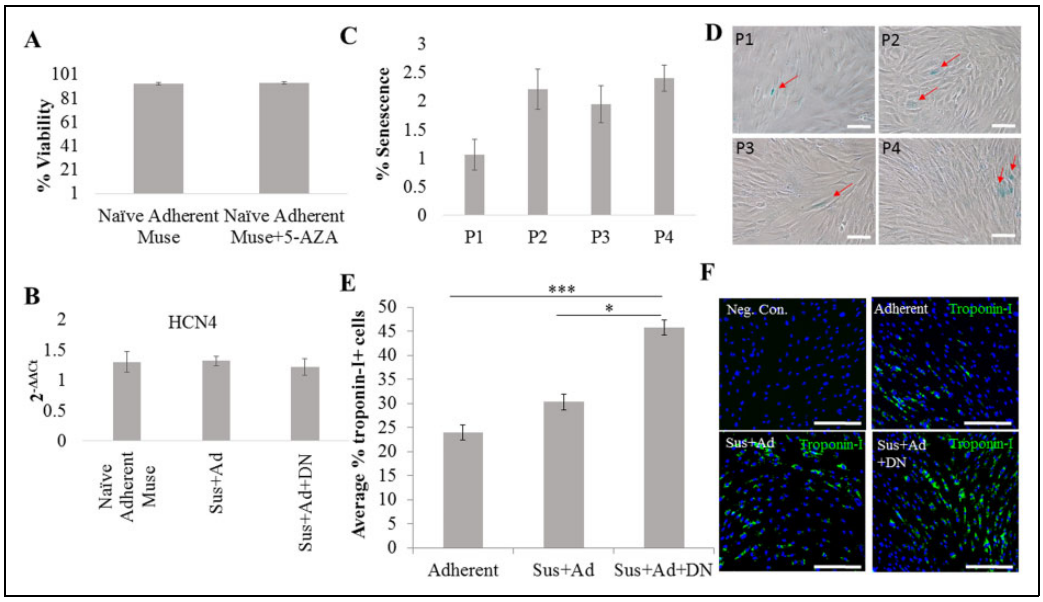

Fig. 3. (A) Trypan blue exclusion showing percentage of viable of Muse cells with or without 5′-azacytidine (5-AZA); (B) quantitative PCR for HCN4 in the naive adherent Muse, Sus+Ad, and Sus+Ad+DN groups; (C) percentage of senescence from passages 1 to 4 MSCs; (D) representative phase contrast photos for β-galactosidase staining from passages 1 to 4 MSCs; (E) average percentage of troponin-I+ cells in the induction groups; (F) representative laser confocal microscopic figures for troponin-I+ cells in the induction groups. *$P < 0.05$, ***$P < 0.001$. Muse cells cultured in adherent, Naive Adherent Muse; Muse cells cultured in suspension in presence of 5′-azacytidine, Naive Suspension Muse + 5-AZA.

comparisons using Microsoft® Excel 2007 software and (GraphPad InStat 3, San Diego, CA, USA) programs.

Results

Pluripotency and DNA Methylation

After isolation, Muse cells had a spindle shape similar to that of mesenchymal cells (Fig. 2A). When they were transferred to suspension culture, Muse cells aggregated to form spheroids (Fig. 2B).

Pluripotency gene expression levels were compared between the naive adherent and naive suspension Muse cells. As shown in Fig. 2C, Pou5f1, Sox2, and Nanog were all substantially upregulated in the naive suspension Muse cells as compared to the naive adherent Muse cells with statistically significant differences. We next tested whether the presence of 5′-AZA, a known factor for DNA demethylation, might further upregulate pluripotency genes in suspension culture. Expression levels of Pou5f1, Sox2, and Nanog in Q-PCR became higher after the addition of 5′-AZA. Notably, Pou5f1 and Nanog showed statistically significant differences ($P < 0.01$; Fig. 2D).

The global DNA methylation level was further investigated among 4 conditions: (1) naive adherent Muse, (2) naive suspension Muse, (3) naive suspension Muse+5-AZA, and (4) suspension Muse+5-AZA/adherent (Fig. 2E). The naive adherent Muse group showed the highest percentage of DNA methylation (1.45%) and was less methylated when these cells were simply cultured in suspension (0.74%), while that was under detection level in the naive suspension Muse+5-AZA group, suggesting that suspension culture combined with 5′-AZA accelerated DNA demethylation. Nonetheless, when the native suspension Muse+5-AZA group was transferred into adherent culture (suspension Muse + 5-AZA/adherent), their DNA methylation percentage increased.

Moreover, the effect of 5′-AZA on Muse cell viability (naive adherent Muse + 5-AZA) was evaluated by the trypan blue exclusion method at 3 d. There was no significant difference in cell viability between the naive adherent Muse with 5′-AZA and without 5′-AZA (Fig. 3A). Based on these findings, we set 3 induction systems, namely, the adherent, Sus+Ad, and Sus+Ad+DN groups in which either adherent or suspension culture were combined with a cocktail of cytokines relevant to cardiac differentiation as shown in Fig. 1. Passage 4 MSCs showed a low percentage of senescence compared to passage 1 (Fig. 3C and D), therefore we used MSCs at passage 4 in our experiment.

DNA Bisulfite Sequencing

Bisulfite sequencing at the Nkx2.5 promoter region showed a significant decrease in the percentage of methylated CpGs in the naive suspension Muse + 5-AZA compared to the naive adherent Muse (Fig. 4A and B). In addition, the percentage of methylated CpGs of the sample 1 induced Muse was significantly lower than that of the naive adherent Muse, with no significant difference in the naive suspension Muse+5-AZA group (Fig. 4B).

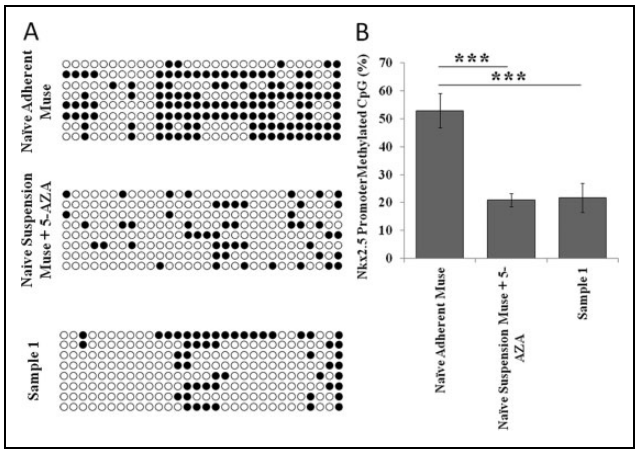

Fig. 4. DNA bisulfite sequencing showing methylation status at Nkx2.5 promoter region. (A) Methylation status of target region at Nkx2.5 promoter with white and black circles representing unmethylated and methylated CpGs, respectively; (B) graphical representation of the percentage of methylated CpG in the naive adherent Muse, naive suspension Muse+5-AZA, and sample 1. ***$P < 0.001$.

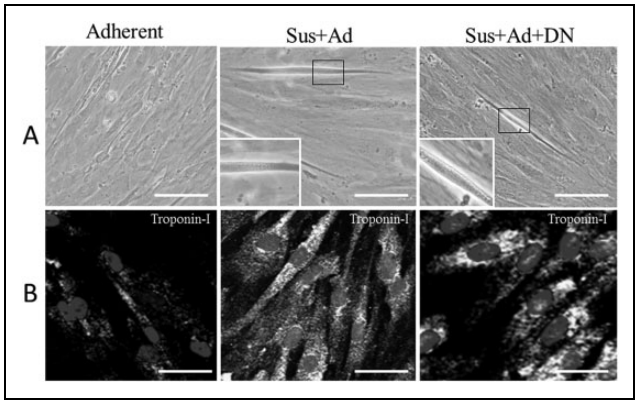

Fig. 5. Striation-like pattern of Muse-derived cardiomyocyte-like cells in Sus+Ad and Sus+Ad+DN at the end point of induction. (A) Phase contrast photos, (B) laser confocal photos of troponin-I stained cells. Scale bar: 100 μm.

Immunocytochemical Analysis

Phase contrast microscopic images at the final time point of each group are shown in Fig. 5A. Cells of the adherent group had morphological features that were different from those of the original naive adherent Muse group (Fig. 2A). Some of the cells of the Sus+Ad and Sus+Ad+DN groups contained striation-like patterns (Fig. 5A). A striation-like pattern was also observed in troponin-I immunocytochemistry in both the Sus+Ad+DN and Sus+Ad groups while that was not evident in the adherent group (Fig. 5B). The results showed 45.7% ± 1.5% troponin-I+ cells in the Sus+Ad+DN group, 30.3% ± 1.6% in the Sus+Ad group, and 24.1% ± 1.6% in the adherent group (Fig. 3E and F).

In double staining with α-actinin and connexin 43, the α-actinin staining pattern was random and not well

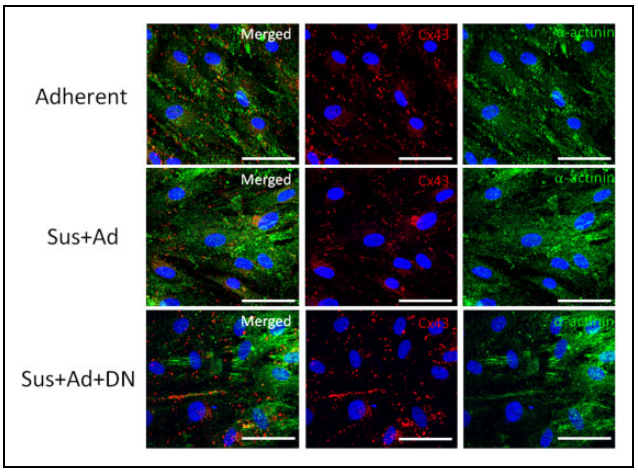

Fig. 6. Laser confocal images of induced Muse double-stained for α-actinin (green) and connexin 43 (red)/diamidino-2-phenylindole (blue) in the adherent, Sus+Ad, and Sus+Ad+DN groups. Scale bar: 100 μm.

organized in the adherent group while that was more organized in the Sus+Ad group (Fig. 6). The Sus+Ad+DN group showed the most organized staining pattern. In all of the 3 groups, connexin 43 seemed to be located mainly at cell–cell contact sites (Fig. 6).

Western Blot Analysis

While all 3 induction groups expressed α-actinin and desmin proteins in Western blot (Fig. 7A), densitometry revealed that the Sus+Ad+DN group showed the highest expression level of α-actinin with statistical significance compared to the adherent group. Furthermore, the Sus-Ad+DN group showed the highest expression level of desmin with significant differences compared with both the adherent and the Sus+Ad groups. On the other hand, the adherent and Sus+Ad groups did not show significantly different expression levels in either marker (Fig. 7B). HCN4—a marker for pacemaker cardimyocytes—was not detected in all groups.

Cardiac Marker Expressions in RT-PCR and Q-PCR

For assessment of cardiac differentiation in each group, RT-PCR analysis was performed at the final time point of each group (Fig. 7C). GATA-4, an early cardiac marker, was not detected in the 3 groups, probably because it is an early cardiac marker and might have been already downregulated at the final time point. Cardiac progenitor markers—Tbx20, ANP, and Nkx2.5—were detected in all 3 groups. Additionally, MLC1a and MLC1v, myosin light chain variants expressed by cardiomyocytes, were detected in all 3 groups. MyoD, a marker for skeletal muscle and not for cardiomyocytes, was not detected in any of the 3 groups.

Even though GATA-4 was not detected by RT-PCR at the final time point of all 3 groups, Q-PCR revealed that GATA-

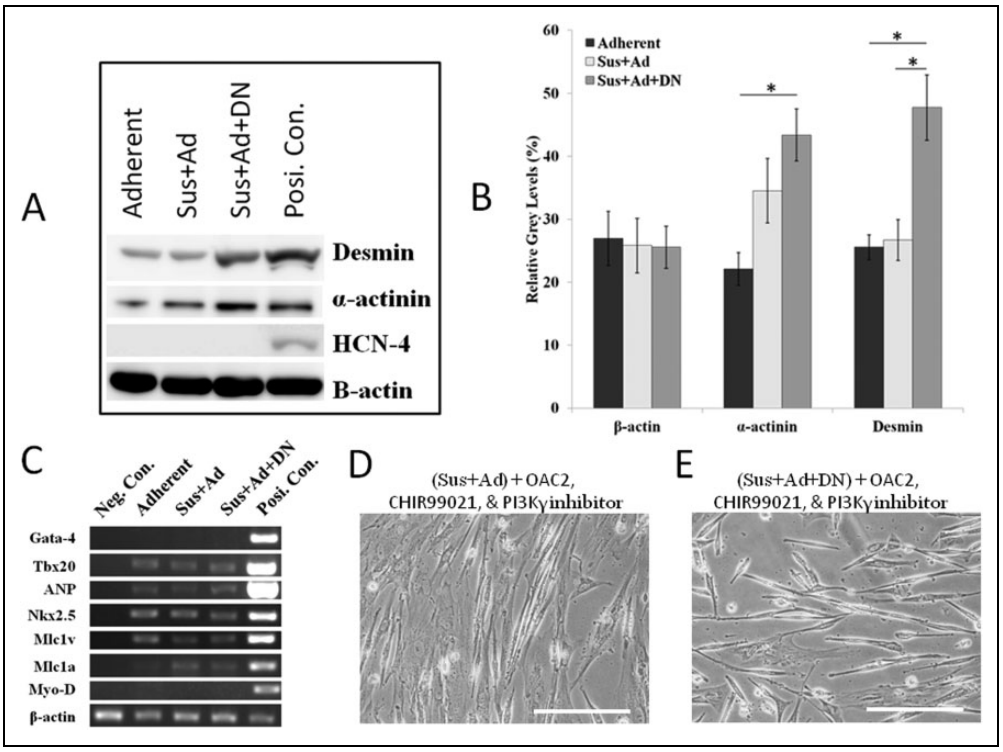

Fig. 7. (A) Western blotting data showing α-actinin and desmin protein expression level of the adherent, Sus+Ad, and Sus+Ad+DN groups. Sus+Ad+DN showed the highest protein expression level among all groups; (B) graphical representation of densitometry Western blotting quantitative data for β-actin, α-actinin, and desmin; (C) RT-PCR analysis of induced Muse stem cells for early and late cardiac markers; (D & E) Addition of OAC2, CHIR99021, and PI3Kγ inhibitor to either the Sus+Ad or the Sus+Ad+DN groups led to increased number of cardiomyocyte-like cells showing striation-like pattern. Scale bar: 100 μm. HCN-4, hyperpolarization activated cyclic nucleotide gated-4; ANP, atrial natriuretic peptide; MLC1v, myosin light chain 1v; MLC1a, myosin light chain 1a;Myo-D, myogenic differentiation antigen; OAC-2, Oct-4 activator; CHIR99021, GSK-3 inhibitor; PI3Kγ, phosphatidyl inositol-3 kinase γ.

4 was not strongly expressed immediately after 7-d incubation with 6 factors (Fig. 8A; corresponding to sample 1 in Fig. 1) but was substantially expressed after inhibition of Wnt and BMP by addition of DKK-1 and Noggin, respectively (the point corresponding to sample 2 in Fig. 1), in the Sus+Ad+DN group (Fig. 8A). However, GATA-4 was not detected at the final time point in any of the 3 groups (Fig. 8A). Expression of α-actinin in Q-PCR was the highest in the Sus+Ad+DN group compared to the other groups (Fig. 8A).

The Sus+Ad group showed the highest expression of MLC2a with statistically significant differences compared with other groups (Fig. 8B). The adherent group showed the lowest expression, which significantly increased in the Sus-Ad+DN group. MLC2a expression was under the detection level in the Sus+Ad+DN(-CT-1) group.

The Sus+Ad+DN group showed the highest expression of MLC2v with statistically significant differences compared with other groups (Fig. 8C). The adherent group showed the lowest expression, which was significantly increased after DKK-1 and Noggin treatment (sample 2) and also in the Sus+Ad group. MLC2v expression of the Sus+Ad+DN group significantly decreased in both the Sus-Ad+DN(-CT-1) and Sus+Ad+DN(-HGF) groups. Furthermore, the expression level of HCN4 in QPCR in the Sus+Ad and Sus+Ad+DN groups was basically the same as that in the naive adherent Muse group (Fig. 3B).

CT-1 Signaling in Cardiac Differentiation Illustrated by Q-PCR

Muse cells induced with either CT-1 only or CT-1/MEKi showed nearly the same α-actinin expression level (Fig. 8D). In contrast, α-actinin expression was abrogated in the CT-1/PI3Ki group. Induction with a GSK3 inhibitor partially suppressed α-actinin expression. However, the expression level was significantly ($P < 0.01$) lower than in either CT-1 only or the presence of a MEK1,2 inhibitor.

We tried adding small molecules known to enhance programming of stem cells. Since the induction was dependent on the PI3K pathway, we thought that inhibition of the PI3Kγ subtype—known to interfere with cardiomyocyte maturation[31]—during last 2 wk of induction might be beneficial. In addition, Oct4 activator; OAC-2 and GSK3 inhibitor; CHIR99021 were added to both the Sus+Ad and Sus+Ad+DN groups on the first week and last two weeks of induction, respectively. These modified protocols showed an increase in the incidence of cells with a striation-like pattern (Fig. 7D&E).

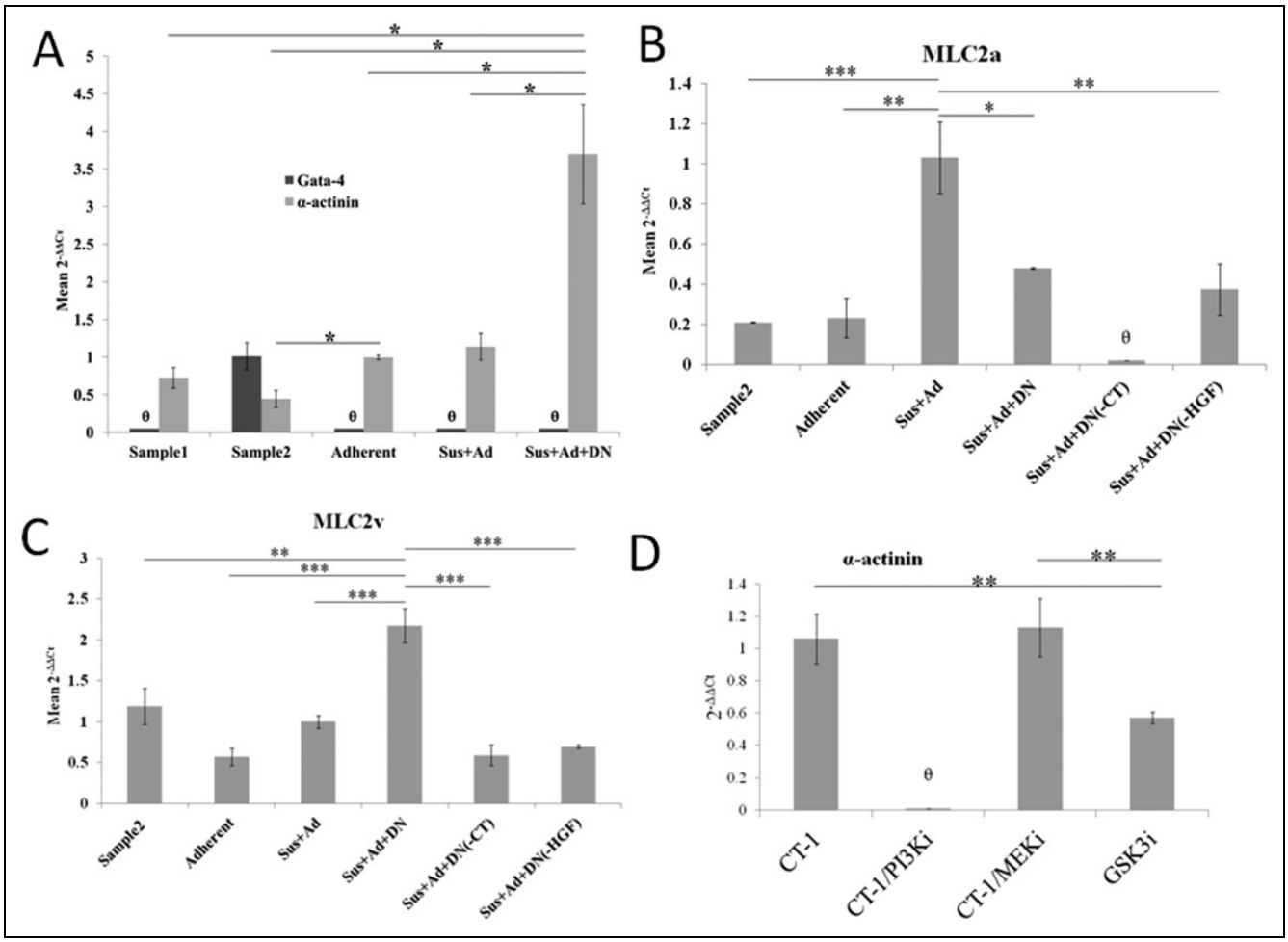

Fig. 8. Q-PCR analysis of cardiac markers. (A) α-actinin and GATA-4 expression in adherent, Sus+Ad, and Sus+Ad+DN groups at the final time point, together with samples 1 and 2; (B) MLC2a and (C) MLC2v expression in adherent, Sus+Ad, and Sus+Ad+DN groups at the final time point, together with sample 2, Sus+Ad+DN without cardiotrophin-1(Sus+Ad+DN(-CT)), and Sus+Ad+DN without hepatocyte growth factor (Sus+Ad+DN(-HGF)); (D) Q-PCR analysis of α-actinin expression in Muse cells induced with either cardiotrophin-1(CT-1), cardiotrophin-1 with Posphatidyl inositol-3 kinase inhibitor (CT-1/PI3Ki), cardiotrophin-1 with mitogen activated protein kinase 1,2 inhibitor (CT-1/MEKi), and glycogen synthetase-3 kinase inhibitor (GSK3i); *$P < 0.05$, **$P < 0.01$, ***$P < 0.001$. θ, expression below the detection level; Q-PCR, quantitative polymerase chain reaction; HGF, hepatocyte growth factor; MLC2a, myosin light chain 2a; MLC2v, myosin light chain 2v.

Discussion

In the present article, we tested 3 protocols for cardiomyocyte induction. Q-PCR analysis of α-actinin, GATA-4, MLC2a, and MLC2v expression as well as Western blot of α-actinin and desmin expression levels were used to compare the efficiency of cardiac differentiation among the 3 protocols. Immunocytochemical analysis confirmed the expression of troponin-I, α-actinin, and connexin 43 proteins. We selected early cardiac markers including Tbx20, GATA-4, Nkx2.5, and ANP as well as late cardiac markers such as MLC1a and MLC1v for RT-PCR assays.

Several attempts to induce MSCs into cardiomyocytes were based on coculture of MSCs with cardiomyocytes rather than cytokine-driven induction.[32-34] In addition, some investigators used a cardiomyocyte extract for induction.[33,35,36] These experimental approaches showed that MSCs have the potential for cardiac differentiation. Nonetheless, the involvement of nonhuman cells or tissue extracts might delay their progression toward clinical applications.

Suspension Culture and 5′-AZA

Some reports suggested that 5′-AZA induces dedifferentiation and enhances cell plasticity in some types of somatic cells[37] and facilitates cardiac differentiation in rat MSCs by inducing DNA demethylation[38]. Regarding suspension culture, Kuroda et al. demonstrated that Muse cell self-renewal and pluripotency become apparent when they are cultured in suspension[4]. We confirmed that suspension culture substantially upregulated the expression level of genes related to pluripotency in Muse cells when compared to adherent Muse cells, and administration of 5′-AZA to suspension culture

further upregulated pluripotency gene expression. These observations are consistent with the data at DNA methylation levels. Suspension plus 5′-AZA reduced DNA methylation levels in Muse cells, whereas the return of these cells to the adherent state reverted the DNA methylation level. Such regulation via epigenetic mechanisms and pluripotency genes may be present in the Sus+Ad and Sus+Ad+DN groups, where both suspension and 5′-AZA were incorporated into the induction procedure, allowing higher expression of α-actinin protein and gene expression levels as compared to the adherent group.

Bisulfite sequencing data were consistent with global methylation data, showing that suspension and 5′-AZA significantly decreased the methylated CpG percentage in the naive suspension Muse +5-AZA group compared to the naive adherent Muse. Moreover, the methylated CpG percentage of sample 1 was still significantly lower than that of the naive adherent Muse group with no significant difference from the naive suspension Muse + 5-AZA group. This shows that the first step of cytokine induction prevented the reversal of DNA methylation that happened upon transfer to adherent culture as shown in the suspension Muse+5-AZA/adherent group global methylation data (Fig. 2E).

Cytokines for Cardiac Differentiation

Several reports have described the induction of cardiomyocyte-like cells from BM-MSCs with various sets of cytokines. Behfar et al. used single-step cytokine induction with TGF-β1, BMP-4, activin A, retinoic acid, bFGF, IGF-1, α-thrombin, and IL-6, assessing the induction effect by means of Nkx2.5 and Mef2c[39]. Siegel et al. used different cytokine cocktails: those containing 5′-AZA, bFGF, vascular endothelial growth factor (VEGF), BMP2, and Noggin and validated differentiation by Q-PCR analysis of troponin-I, α-actinin, and myosin light chain. Although cardiac lineage genes were detected, those authors stated that the cells did not differentiate into mature functional cardiomyocytes[40]. Shim et al. used insulin, dexamethasone, and ascorbic acid and reported cardiomyocyte-like cells with the formation of a striation-like pattern[41].

Indeed, the cardiac specification is a complex process of differentiation that is controlled by several cytokines in a context-dependent manner. A combination of TGF-β1 and BMP4 induces differentiation toward the mesoendodermal lineage via Smad2/3 and Smad1/5/8, respectively, whereas either of them alone does not work sufficiently[19,42]. BMP/Smads facilitate expression of cardiac progenitor cell markers such as GATA-4 and Mef2, whereas Wnt/β-catenin induces Nkx2.5 and Islet-1[43]. In our protocol for the Sus+Ad and Sus+Ad+DN groups, TGF-β1, BMP2, BMP4, activin A, Wnt3a, and bFGF might have synergistically activated cardiac differentiation of Muse cells, which were strongly potentiated by suspension culture plus 5′-AZA. What is unique to the Sus+Ad+DN group is that the protocol contains an extra step of DKK-1 and Noggin incubation. Some studies on murine cardiac development showed that Noggin, a BMP pathway blocker, promotes the cardiac commitment of meso/endodermal lineage cells[44]. Long-term exposure to Noggin halts cardiac development in mice[45]. Wnt/β-catenin signaling during early development facilitates mesodermal cell differentiation into cardiomyocytes rather than a hematopoietic lineage; however, at late developmental stages, it has the opposite effect[46]. DKK-1, a Wnt pathway blocker, promotes specification of cardiac precursors in the anterolateral mesoderm that forms the cardiac crescent[47]. Consequently, effects of DKK-1 and Noggin on cardiac development depend on developmental status. These data suggest that the Sus+Ad+DN protocol is rationally designed as compared to the other 2 protocols.

CT-1 and HGF might be key factors for the late step induction in our protocols. When the Sus+Ad+DN goup induction was performed in the absence of either CT-1 or HGF, MLC2a and MLC2v gene expression was substantially lowered; MLC2a expression was even under the detection level in the Sus+Ad+DN(-CT) group. Moreover, CT-1 cardiac induction is mainly dependent on the PI3K pathway since α-actinin gene expression level became undetectable in the presence of the PI3K inhibitor. The importance of GSK3 inhibition—a downstream signaling pathway of PI3K—in cardiac programming has been described previously[48]. However, GSK3 inhibition yielded a lower α-actinin gene expression level compared to CT-1. This may suggest that GSK3 inhibition is not the only downstream pathway of PI3K responsible for cardiac programming.

Cardiac Marker Expression in Induced Muse Cells

All of the groups expressed cardiac progenitor markers: Nkx2.5, Tbx20, and ANP. GATA-4 is an early marker of cardiac development, the expression of which is observed before linear heart development[49]. Although GATA-4 expression could not be detected at the final time point of any of the 3 induction groups, Q-PCR revealed that the cells in the Sus+Ad+DN group expressed GATA-4 only after DKK-1 and Noggin induction (sample 2). The same group showed the highest α-actinin expression at the final time point when compared to the same time point in the adherent or Sus+Ad groups. These results may eventually help to explain why DKK-1 and Noggin promote maturation of cardiac progenitor cells, causing an increase in the expression of α-actinin at the final time point of induction.

All groups tested negative for Myo-D; this finding suggested that all the induced cells were not skeletal muscle cells[50].

There was a gradual increase in α-actinin protein expression in the Sus+Ad+DN and adherent groups, showing the highest and lowest expression, respectively. Also, the Sus+Ad+DN showed a higher desmin protein level compared to other groups. However, none of the groups expressed the pacemaker cardiomyocyte marker HCN4 as shown in the Western blot.

Troponin-I positive cells with a striation-like pattern were regularly organized in the Sus+Ad and Sus+Ad+DN groups and were positive for α-actinin which is characteristic of Z line responsible for actin–myosin cross-linking[51]. Additionally, the striations were positive for troponin-I: the troponin subunit responsible for binding the troponin–tropomyosin complex to actin[52]. The presence of connexin 43 is suggestive of functional characteristics of the Muse cells converted into cardiomyocyte-like cells. Preda et al. reported that IGF-1 and bFGF, both of which were included in our protocol, enhance connexin 43 mRNA and protein expression in murine BM-MSCs[53].

Ventricular and Atrial Subtypes

Directed atrial and ventricular differentiation of human[54] or murine[55] ESCs has been shown previously. Nonetheless, atrial and ventricular differentiation from MSCs have never been attempted before. The expression pattern of different variants of myosin light is used to differentiate atrial and ventricular cardiomyocytes. MLC2a is expressed throughout the linear heart during cardiac development, then becomes restricted to fetal atria[56,57]. On the other hand, MLC2v is considered as a marker for ventricular specification in the linear heart tube and adult heart[58].

The adherent group showed the lowest MLC2a or MLC2v gene expression level. This result is suggestive of incomplete or weak differentiation of Muse cells toward either atrial or ventricular cardiomyocytes. On the other hand, the Sus+Ad group showed the highest expression level of MLC2a. This expression profile indicates directed differentiation toward atrial cardiomyocytes. Sample2—which is indicative of a DKK-1/Noggin effect—showed significantly higher MLC2v gene expression compared to the adherent group. The Sus-Ad+DN group showed the highest MLC2v gene expression level among all groups, suggesting directed differentiation toward ventricular cardiomycytes.

The induced Muse cells in our article—particularly the Sus+Ad+DN group—expressed major markers of mature cardiomyocytes. On the other hand, they did not show spontaneous beating nor did they express the pacemaker cardiomyocyte marker HCN4 as shown by Western blotting and Q-PCR. It is suggested that the induction method described in our study preferentially induced Muse cells into working cardiomyocytes but not into pacemaker cells, or that Muse cells have a lower potential for differentiation into pacemaker cells rather than into working cardiomyocytes. Usually, mature working cardiomyocytes do not spontaneously beat in the absence of the pacemaker cell stimulus[59,60]. This might partly explain the lack of spontaneous beating in the induced cells. From another view point, this might be beneficial for regenerative medicine, since the induced cells will simply follow the original rhythm of the host pacemaker cells avoiding ectopic foci of contraction that may lead to arrhythmias[61].

Embryonic and induced pluripotent stem cells have been the focus of cardiac regeneration studies because of their high pluripotency and the ability to stably proliferate in vitro into a large number of cells. However, their clinical applications are still under scrutiny, hindered by their tumorigenicity[62] and ethical issues associated with ESCs[63]. We used Muse cells at a low in vitro passage. This is because high growth in vitro may induce senescence that impairs the therapeutic potential of these cells. Indeed, the failure in some BM-MSC-based therapies has to be ascribed to the use of cultures with a high percentage of senescent cells. Currently, several investigators recommend evaluation of the senescent cell percentage in samples that have to be used for clinical purposes[64,65]. Being nontumorigenic and available from easily accessible sources (such as bone marrow aspirates or adipose tissue), Muse cells seem to be suitable for clinical applications[66].

Conclusion

In the present article, we showed a system for in vitro cardiac lineage induction of Muse cells. In addition, the directed differentiation toward human atrial or ventricular cardiomyocyte-like cells in a simple 3- or 4-step induction procedure is described. Neither the Muse cell collection nor the induction method involved any genetic manipulations or unethical procedures. We believe that this article would be beneficial for clinical applications in cardiac diseases including personalized regenerative treatment.

Ethical Approval

The statement of Ethical Approval is not applicable for this article.

Statement of Human and Animal Rights

This article does not contain any studies with human or animal subjects and Statement of Human and Animal Rights is not applicable.

Statement of Informed Consent

There are no human subjects in this article and informed consent is not applicable.

Declaration of Conflicting Interests

The author(s) declared the following potential conflicts of interest with respect to the research, authorship, and/or publication of this article: Yoshihiro Kushida, Shohei Wakao and Mari Dezawa are affiliated with the Department of Stem Cell Biology and Histology at Tohoku University Graduate School of Medicine, which is party to a codevelopment agreement with Life Science Institute, Inc. (LSII). Mari Dezawa and Shohei Wakao have a patent Muse cells and isolation method thereof licensed to LSII.

Funding

The author(s) received no financial support for the research, authorship, and/or publication of this article.

References

1. Murata M, Tohyama S, Fukuda K. Impacts of recent advances in cardiovascular regenerative medicine on clinical therapies and drug discovery. Pharmacol Ther. 2010;126(2):109–118.

2. Kuroda Y, Wakao S, Kitada M, Murakami T, Nojima M, Dezawa M. Isolation, culture and evaluation of multilineage-differentiating stress-enduring (Muse) cells. Nat Protoc. 2013; 8(7):1391–1415.
3. Pittenger MF, Mackay AM, Beck SC, Jaiswal RK, Douglas R, Mosca JD, Moorman MA, Simonetti DW, Craig S, Marshak DR. Multilineage potential of adult human mesenchymal stem cells. Science. 1999;284(5411):143–147.
4. Kuroda Y, Kitada M, Wakao S, Nishikawa K, Tanimura Y, Makinoshima H, Goda M, Akashi H, Inutsuka A, Niwa A, et al. Unique multipotent cells in adult human mesenchymal cell populations. Proc Natl Acad Sci U S A. 2010;107(19): 8639–8643.
5. Tsuchiyama K, Wakao S, Kuroda Y, Ogura F, Nojima M, Sawaya N, Yamasaki K, Aiba S, Dezawa M. Functional melanocytes are readily reprogrammable from multilineage-differentiating stress-enduring (muse) cells, distinct stem cells in human fibroblasts. J Invest Dermatol. 2013;133(10): 2425–2435.
6. Kinoshita K, Kuno S, Ishimine H, Aoi N, Mineda K, Kato H, Doi K, Kanayama K, Feng J, Mashiko T, et al. Therapeutic potential of adipose-derived SSEA-3-positive muse cells for treating diabetic skin ulcers. Stem Cells Transl Med. 2015; 4(2):146–155.
7. Uchida H, Morita T, Niizuma K, Kushida Y, Kuroda Y, Wakao S, Sakata H, Matsuzaka Y, Mushiake H, Tominaga T, et al. Transplantation of unique subpopulation of fibroblasts, muse cells, ameliorates experimental stroke possibly via robust neuronal differentiation. Stem Cells. 2016;34(1): 160–173.
8. Uchida H, Niizuma K, Kushida Y, Wakao S, Tominaga T, Borlongan CV, Dezawa M. Human muse cells reconstruct neuronal circuitry in subacute lacunar stroke model. Stroke. 2017; 48(2):428–435.
9. Katagiri H, Kushida Y, Nojima M, Kuroda Y, Wakao S, Ishida K, Endo F, Kume K, Takahara T, Nitta H, et al. A Distinct subpopulation of bone marrow mesenchymal stem cells, muse cells, directly commit to the replacement of liver components. Am J Transplant. 2016;16(2):468–483.
10. Iseki M, Kushida Y, Wakao S, Akimoto T, Mizuma M, Motoi F, Asada R, Shimizu S, Unno M, Chazenbalk G, et al. Human Muse cells, non-tumorigenic pluripotent-like stem cells, have the capacity for liver regeneration by specific homing and replenishment of new hepatocytes in liver fibrosis mouse model. Cell Transplant. 2017;26(5):821–840.
11. Ogura F, Wakao S, Kuroda Y, Tsuchiyama K, Bagheri M, Heneidi S, Chazenbalk G, Aiba S, Dezawa M. Human adipose tissue possesses a unique population of pluripotent stem cells with nontumorigenic and low telomerase activities: potential implications in regenerative medicine. Stem Cells Dev. 2014; 23(7):717–728.
12. Heneidi S, Simerman AA, Keller E, Singh P, Li X, Dumesic DA, Chazenbalk G. Awakened by cellular stress: isolation and characterization of a novel population of pluripotent stem cells derived from human adipose tissue. PLoS One. 2013;8(6): e64752.
13. Wakao S, Kitada M, Kuroda Y, Shigemoto T, Matsuse D, Akashi H, Tanimura Y, Tsuchiyama K, Kikuchi T, Goda M, et al. Multilineage-differentiating stress-enduring (Muse) cells are a primary source of induced pluripotent stem cells in human fibroblasts. Proc Natl Acad Sci U S A. 2011;108(24): 9875–9880.
14. Gimeno ML, Fuertes F, Barcala Tabarrozzi AE, Attorressi AI, Cucchiani R, Corrales L, Oliveira TC, Sogayar MC, Labriola L, Dewey RA, et al. Pluripotent nontumorigenic adipose tissue-derived muse cells have immunomodulatory capacity mediated by transforming growth factor-beta1. Stem Cells Transl Med. 2017;6(1):161–173.
15. Moyzis AG, Sadoshima J, Gustafsson AB. Mending a broken heart: the role of mitophagy in cardioprotection. Am J Physiol Heart Circ Physiol. 2015;308(3): H183–H192.
16. Hwang PM, Sykes BD. Targeting the sarcomere to correct muscle function. Nat Rev Drug Discov. 2015;14(5):313–328.
17. Jeyaraman MM, Srisakuldee W, Nickel BE, Kardami E. Connexin43 phosphorylation and cytoprotection in the heart. Biochim Biophys Acta. 2012;1818(8):2009–2013.
18. Li Z, Chen YG. Functions of BMP signaling in embryonic stem cell fate determination. Exp Cell Res. 2013;319(2):113–119.
19. Beyer TA, Narimatsu M, Weiss A, David L, Wrana JL. The TGFbeta superfamily in stem cell biology and early mammalian embryonic development. Biochim Biophys Acta. 2013; 1830(2):2268–2279.
20. Yu P, Pan G, Yu J, Thomson JA. FGF2 sustains NANOG and switches the outcome of BMP4-induced human embryonic stem cell differentiation. Cell Stem Cell. 2011;8(3):326–334.
21. Pennica D, King KL, Shaw KJ, Luis E, Rullamas J, Luoh SM, Darbonne WC, Knutzon DS, Yen R, Chien KR, et al. Expression cloning of cardiotrophin 1, a cytokine that induces cardiac myocyte hypertrophy. Proc Natl Acad Sci U S A. 1995;92(4): 1142–1146.
22. Ruixing Y, Jinzhen W, Dezhai Y, Jiaquan L. Cardioprotective role of cardiotrophin-1 gene transfer in a murine model of myocardial infarction. Growth Factors. 2007;25(4):286–294.
23. Bartunek J, Behfar A, Dolatabadi D, Vanderheyden M, Ostojic M, Dens J, El Nakadi B, Banovic M, Beleslin B, Vrolix M, et al. Cardiopoietic stem cell therapy in heart failure: the C-CURE (Cardiopoietic stem Cell therapy in heart failURE) multicenter randomized trial with lineage-specified biologics. J Am Coll Cardiol. 2013;61(23):2329–2338.
24. Mascheck L, Sharifpanah F, Tsang SY, Wartenberg M, Sauer H. Stimulation of cardiomyogenesis from mouse embryonic stem cells by nuclear translocation of cardiotrophin-1. Int J Cardiol. 2015;193:23–33.
25. Peran M, Marchal JA, Lopez E, Jimenez-Navarro M, Boulaiz H, Rodriguez-Serrano F, Carrillo E, Sanchez-Espin G, de Teresa E, Tosh D, et al. Human cardiac tissue induces transdifferentiation of adult stem cells towards cardiomyocytes. Cytotherapy. 2010;12(3):332–337.
26. Laumen H, Brunner C, Greiner A, Wirth T. Myosin light chain 1 atrial isoform (MLC1A) is expressed in pre-B cells under control of the BOB.1/OBF.1 coactivator. Nucleic Acids Res. 2004;32(4):1577–1583.

27. Otaka S, Nagura S, Koike C, Okabe M, Yoshida T, Fathy M, Yanagi K, Misaki T, Nikaido T. Selective isolation of nanog-positive human amniotic mesenchymal cells and differentiation into cardiomyocytes. Cell Reprogram. 2013;15(1):80–91.
28. Frascella E, Rosolen A. Detection of the MyoD1 transcript in rhabdomyosarcoma cell lines and tumor samples by reverse transcription polymerase chain reaction. Am J Pathol. 1998; 152(2):577–583.
29. Sanchez-Freire V, Lee AS, Hu S, Abilez OJ, Liang P, Lan F, Huber BC, Ong SG, Hong WX, Huang M, et al. Effect of human donor cell source on differentiation and function of cardiac induced pluripotent stem cells. J Am Coll Cardiol. 2014;64(5):436–448.
30. Davis DR, Kizana E, Terrovitis J, Barth AS, Zhang Y, Smith RR, Miake J, Marban E. Isolation and expansion of functionally-competent cardiac progenitor cells directly from heart biopsies. J Mol Cell Cardiol. 2010;49(2):312–321.
31. Shiojima I, Walsh K. Regulation of cardiac growth and coronary angiogenesis by the Akt/PKB signaling pathway. Genes Dev. 2006;20(24):3347–3365.
32. Wang T, Xu Z, Jiang W, Ma A. Cell-to-cell contact induces mesenchymal stem cell to differentiate into cardiomyocyte and smooth muscle cell. Int J Cardiol. 2006;109(1):74–81.
33. Rangappa S, Entwistle JW, Wechsler AS, Kresh JY. Cardiomyocyte-mediated contact programs human mesenchymal stem cells to express cardiogenic phenotype. J Thorac Cardiovasc Surg. 2003;126(1):124–132.
34. Pijnappels DA, Schalij MJ, Ramkisoensing AA, van Tuyn J, de Vries AA, van der Laarse A, Ypey DL, Atsma DE. Forced alignment of mesenchymal stem cells undergoing cardiomyogenic differentiation affects functional integration with cardiomyocyte cultures. Circ Res. 2008;103(2):167–176.
35. Pham TL, Nguyen TT, Van Bui A, Nguyen MT, Van Pham P. Fetal heart extract facilitates the differentiation of human umbilical cord blood-derived mesenchymal stem cells into heart muscle precursor cells. Cytotechnology. 2016;68(4): 645–658.
36. Ge D, Liu X, Li L, Wu J, Tu Q, Shi Y, Chen H. Chemical and physical stimuli induce cardiomyocyte differentiation from stem cells. Biochem Biophys Res Commun. 2009;381(3): 317–321.
37. Chandrakanthan V, Yeola A, Kwan JC, Oliver RA, Qiao Q, Kang YC, Zarzour P, Beck D, Boelen L, Unnikrishnan A, et al. PDGF-AB and 5-Azacytidine induce conversion of somatic cells into tissue-regenerative multipotent stem cells. Proc Natl Acad Sci U S A. 2016;113(16): E2306–E2315.
38. Naeem N, Haneef K, Kabir N, Iqbal H, Jamall S, Salim A. DNA methylation inhibitors, 5-azacytidine and zebularine potentiate the transdifferentiation of rat bone marrow mesenchymal stem cells into cardiomyocytes. Cardiovasc Ther. 2013; 31(4):201–209.
39. Behfar A, Yamada S, Crespo-Diaz R, Nesbitt JJ, Rowe LA, Perez-Terzic C, Gaussin V, Homsy C, Bartunek J, Terzic A. Guided cardiopoiesis enhances therapeutic benefit of bone marrow human mesenchymal stem cells in chronic myocardial infarction. J Am Coll Cardiol. 2010;56(9):721–734.
40. Siegel G, Krause P, Wohrle S, Nowak P, Ayturan M, Kluba T, Brehm BR, Neumeister B, Kohler D, Rosenberger P, et al. Bone marrow-derived human mesenchymal stem cells express cardiomyogenic proteins but do not exhibit functional cardiomyogenic differentiation potential. Stem Cells Dev. 2012; 21(13):2457–2470.
41. Shim WS, Jiang S, Wong P, Tan J, Chua YL, Tan YS, Sin YK, Lim CH, Chua T, Teh M, et al. Ex vivo differentiation of human adult bone marrow stem cells into cardiomyocyte-like cells. Biochem Biophys Res Commun. 2004;324(2): 481–488.
42. Greber B, Lehrach H, Adjaye J. Control of early fate decisions in human ES cells by distinct states of TGFbeta pathway activity. Stem Cells Dev. 2008;17(6):1065–1077.
43. Klaus A, Muller M, Schulz H, Saga Y, Martin JF, Birchmeier W. Wnt/beta-catenin and Bmp signals control distinct sets of transcription factors in cardiac progenitor cells. Proc Natl Acad Sci U S A. 2012;109(27):10921–10926.
44. Yuasa S, Itabashi Y, Koshimizu U, Tanaka T, Sugimura K, Kinoshita M, Hattori F, Fukami S, Shimazaki T, Ogawa S, et al. Transient inhibition of BMP signaling by Noggin induces cardiomyocyte differentiation of mouse embryonic stem cells. Nat Biotechnol. 2005;23(5):607–611.
45. Simmons O, Snider P, Wang J, Schwartz RJ, Chen Y, Conway SJ. Persistent Noggin arrests cardiomyocyte morphogenesis and results in early in utero lethality. Dev Dyn. 2015;244(3): 457–467.
46. Naito AT, Shiojima I, Akazawa H, Hidaka K, Morisaki T, Kikuchi A, Komuro I. Developmental stage-specific biphasic roles of Wnt/beta-catenin signaling in cardiomyogenesis and hematopoiesis. Proc Natl Acad Sci U S A. 2006;103(52): 19812–19817.
47. Cohen ED, Tian Y, Morrisey EE. Wnt signaling: an essential regulator of cardiovascular differentiation, morphogenesis and progenitor self-renewal. Development. 2008;135(5):789–798.
48. Woulfe KC, Gao E, Lal H, Harris D, Fan Q, Vagnozzi R, DeCaul M, Shang X, Patel S, Woodgett JR, et al. Glycogen synthase kinase-3beta regulates post-myocardial infarction remodeling and stress-induced cardiomyocyte proliferation in vivo. Circ Res. 2010;106(10):1635–1645.
49. Svensson EC, Tufts RL, Polk CE, Leiden JM. Molecular cloning of FOG-2: a modulator of transcription factor GATA-4 in cardiomyocytes. Proc Natl Acad Sci U S A. 1999;96(3): 956–961.
50. Scrable HJ, Johnson DK, Rinchik EM, Cavenee WK. Rhabdomyosarcoma-associated locus and MYOD1 are syntenic but separate loci on the short arm of human chromosome 11. Proc Natl Acad Sci U S A. 1990;87(6):2182–2186.
51. Liu H, Shao Y, Qin W, Runyan RB, Xu M, Ma Z, Borg TK, Markwald R, Gao BZ. Myosin filament assembly onto myofibrils in live neonatal cardiomyocytes observed by TPEF-SHG microscopy. Cardiovasc Res. 2013;97(2):262–270.
52. Zhang P, Kirk JA, Ji W, dos Remedios CG, Kass DA, Van Eyk JE, Murphy AM. Multiple reaction monitoring to identify site-specific troponin I phosphorylated residues in the failing human heart. Circulation. 2012;126(15):1828–18237.

53. Preda MB, Rosca AM, Tutuianu R, Burlacu A. Pre-stimulation with FGF-2 increases in vitro functional coupling of mesenchymal stem cells with cardiac cells. Biochem Biophys Res Commun. 2015;464(2):667–673.
54. Zhang Q, Jiang J, Han P, Yuan Q, Zhang J, Zhang X, Xu Y, Cao H, Meng Q, Chen L, et al. Direct differentiation of atrial and ventricular myocytes from human embryonic stem cells by alternating retinoid signals. Cell Res. 2011;21(4): 579–587.
55. Hidaka K, Lee JK, Kim HS, Ihm CH, Iio A, Ogawa M, Nishikawa S, Kodama I, Morisaki T. Chamber-specific differentiation of Nkx2.5-positive cardiac precursor cells from murine embryonic stem cells. FASEB J. 2003;17(6):740–742.
56. Kubalak SW, Miller-Hance WC, O'Brien TX, Dyson E, Chien KR. Chamber specification of atrial myosin light chain-2 expression precedes septation during murine cardiogenesis. J Biol Chem. 1994;269(24):16961–16970.
57. Hailstones D, Barton P, Chan-Thomas P, Sasse S, Sutherland C, Hardeman E, Gunning P. Differential regulation of the atrial isoforms of the myosin light chains during striated muscle development. J Biol Chem. 1992;267(32):23295–23300.
58. O'Brien TX, Lee KJ, Chien KR. Positional specification of ventricular myosin light chain 2 expression in the primitive murine heart tube. Proc Natl Acad Sci U S A. 1993;90(11): 5157–5161.
59. Satin J, Kehat I, Caspi O, Huber I, Arbel G, Itzhaki I, Magyar J, Schroder EA, Perlman I, Gepstein L. Mechanism of spontaneous excitability in human embryonic stem cell derived cardiomyocytes. J Physiol. 2004;559(pt 2):479–496.
60. DeHaan RL, Gottlieb SH. The electrical activity of embryonic chick heart cells isolated in tissue culture singly or in interconnected cell sheets. J Gen Physiol. 1968;52(4): 643–665.
61. Chong JJ, Yang X, Don CW, Minami E, Liu YW, Weyers JJ, Mahoney WM, Van Biber B, Cook SM, Palpant NJ, et al. Human embryonic-stem-cell-derived cardiomyocytes regenerate non-human primate hearts. Nature. 2014;510(7504):273–277.
62. Ben-David U, Benvenisty N. The tumorigenicity of human embryonic and induced pluripotent stem cells. Nat Rev Cancer. 2011;11(4):268–277.
63. Johnson MH. Human ES cells and a blastocyst from one embryo: exciting science but conflicting ethics? Cell Stem Cell. 2008;2(2):103–104.
64. Galipeau J. The mesenchymal stromal cells dilemma—Does a negative phase III trial of random donor mesenchymal stromal cells in steroid-resistant graft-versus-host disease represent a death knell or a bump in the road? Cytotherapy. 2013; 15(1):2–8.
65. Capasso S, Alessio N, Squillaro T, Di Bernardo G, Melone MA, Cipollaro M, Peluso G, Galderisi U. Changes in autophagy, proteasome activity and metabolism to determine a specific signature for acute and chronic senescent mesenchymal stromal cells. Oncotarget. 2015;6(37): 39457–39468.
66. Kuroda Y, Dezawa M. Mesenchymal stem cells and their subpopulation, pluripotent muse cells, in basic research and regenerative medicine. Anat Rec (Hoboken). 2014;297(1): 98–110.